

1  
2  
3  
4  
5  
6  
7  
8  
9  
10  
11  
12  
13  
14  
15  
16  
17  
18  
19  
20  
21  
22  
23  
24  
25  
26  
27  
28  
29  
30  
31  
32  
33  
34  
35  
36  
37  
38  
39  
40  
41  
42  
43  
44  
45  
46

## **Myofilament Glycation in Diabetes Reduces Contractility by Inhibiting Tropomyosin Movement, is Rescued by cMyBPC Domains**

Maria Papadaki<sup>1</sup>, Theerachat Kampaengsri<sup>1</sup>, Samantha K. Barrick<sup>2</sup>,  
Stuart G. Campbell<sup>3</sup>, Dirk von Lewinski<sup>4</sup>, Peter P. Rainer<sup>4</sup>, Samantha P. Harris<sup>5</sup>,  
Michael J. Greenberg<sup>2</sup>, Jonathan A. Kirk<sup>1</sup>†

<sup>1</sup> Department of Cell and Molecular Physiology, Loyola University of Chicago,  
Maywood, Illinois, USA

<sup>2</sup> Department of Biochemistry and Molecular Biophysics, Washington University in St  
Louis, St Louis, Missouri, USA

<sup>3</sup> Department of Bioengineering, Yale University, New Haven, Connecticut, USA

<sup>4</sup> Division of Cardiology, Medical University of Graz, Graz, Austria

<sup>5</sup> Department of Cellular and Molecular Medicine, The University of Arizona, Tucson,  
Arizona, USA

† Corresponding Author  
Jonathan A. Kirk, Ph.D.  
Department of Cell and Molecular Physiology  
Loyola University Chicago Stritch School of Medicine  
Center for Translational Research, Room 522  
2160 S. First Ave.  
Maywood, IL 60153  
Ph: 708-216-6348  
Email: [jkirk2@luc.edu](mailto:jkirk2@luc.edu)

Total Word Count: 7706

Figures: 7

47

## **Abstract**

48

49

50

51

52

53

54

55

56

57

58

59

60

61

62

63

64

65

66

67

68

69

70

71

72

73 Word Count: 249/250

74

75

76

77

Diabetes doubles the risk of developing heart failure (HF). As the prevalence of diabetes grows, so will HF unless the mechanisms connecting these diseases can be identified. Methylglyoxal (MG) is a glycolysis by-product that forms irreversible modifications on lysine and arginine, called glycation. We previously found that myofilament MG glycation causes sarcomere contractile dysfunction and is increased in patients with diabetes and HF. The aim of this study was to discover the molecular mechanisms by which MG glycation of myofilament proteins cause sarcomere dysfunction and to identify therapeutic avenues to compensate. In humans with type 2 diabetes without HF, we found increased glycation of sarcomeric actin compared to non-diabetics and it correlated with decreased calcium sensitivity. Depressed calcium sensitivity is pathogenic for HF, therefore myofilament glycation represents a promising therapeutic target to inhibit the development of HF in diabetics. To identify possible therapeutic targets, we further defined the molecular actions of myofilament glycation. Skinned myocytes exposed to 100  $\mu$ M MG exhibited decreased calcium sensitivity, maximal calcium-activated force, and crossbridge kinetics. Replicating MG's functional effects using a computer simulation of sarcomere function predicted simultaneous decreases in tropomyosin's blocked-to-closed rate transition and crossbridge duty cycle were consistent with all experimental findings. Stopped-flow experiments and ATPase activity confirmed MG decreased the blocked-to-closed transition rate. Currently, no therapeutics target tropomyosin, so as proof-of-principal, we used a n-terminal peptide of myosin-binding protein C, previously shown to alter tropomyosin's position on actin. C0C2 completely rescued MG-induced calcium desensitization, suggesting a possible treatment for diabetic HF.

Keywords: Myofilament glycation, diabetes, myBPC C0C2, tropomyosin

78

## Abbreviations

79

80 AG: Aminoguanidine

81 AGE: Advanced Glycation Endproducts

82 cMyBPC: cardiac myosin binding protein C

83  $f$ : myosin binding rate

84  $F_{\max}$ : maximal calcium-activated force

85  $g_{xb}$ : myosin detachment rate

86 HF: Heart Failure

87  $k$ : ATP detachment rate constant

88  $K_B$ : blocked-to-closed rate transition

89  $k_{tr}$ : rate of force redevelopment

90 LV: Left Ventricle

91 MG: Methylglyoxal

92 OM: Omecamtiv Mecarbil

93

94

95

96

## **Introduction**

97 Almost half a billion people worldwide have type 2 diabetes mellitus (T2DM), a figure  
98 that is expected to increase by ~40% within 25 years [1]. Diabetes doubles the risk  
99 of developing heart failure [2, 3], independent of the effect on microvascular disease  
100 and hypertension. Left unchecked, the rapid expansion of diabetes will result in an  
101 explosion of heart failure cases. Therefore, it is critical that we discover the  
102 underlying molecular mechanisms that link these two conditions so they might be  
103 targeted therapeutically. We previously reported that one such link is likely mediated  
104 by methylglyoxal (MG) [4], a reactive carbonyl species that is formed from the  
105 degradation of triose phosphates [5] during glycolysis. MG can rapidly and  
106 irreversibly react with arginine and lysine amino acids on proteins [6], a process  
107 called glycation. Glycated proteins are known as advanced glycation end-products  
108 (AGE), and can bind to Receptors of AGE on the cell surface [7], inducing a  
109 signalling cascade resulting in oxidative damage and inflammation [8]. However, it is  
110 also possible for glycation of these residues to act as post-translational modifications  
111 that directly alter protein function, which is the mechanism explored in this study.

112 In recent years we and others have provided evidence that methylglyoxal may  
113 play a role in the development of heart failure [7, 9] through glycation of intracellular  
114 proteins involved in excitation-contraction coupling. For example, methylglyoxal can  
115 react with Ryanodine Receptor and SERCA in the hearts of type I diabetic rats and  
116 alter intracellular calcium handling [10, 11]. Our previous work, however, was the first  
117 to make the connection in humans, showing that MG modifications were increased in  
118 the cardiac myofilament of patients who had diabetes and heart failure, but not in  
119 heart failure patients without diabetes or healthy patients [4]. These MG  
120 modifications, occurring primarily on actin and myosin, reduced cardiomyocyte  
121 myofilament calcium sensitivity and maximal calcium-activated force [4]. However,  
122 whether MG modifications precede the development of overt systolic dysfunction,  
123 and thus represent a possible cause of increased heart failure risk in diabetic  
124 patients, is unknown. Genetic mutations in sarcomere proteins that reduce calcium  
125 sensitivity are a cause of cardiomyopathy and heart failure [12]. Thus, if myofilament  
126 glycation is elevated by diabetes and similarly reduce calcium sensitivity, they are  
127 likely pathogenic for the development of heart failure.

128 Since methylglyoxal modifications are irreversible, there are two possible  
129 approaches to correct the dysfunction: 1) decrease MG levels so these harmful

130 adducts are not formed in the first place, or 2) identify treatments that can  
131 compensate for the dysfunction despite the continued presence of the MG  
132 modifications. Genetic approaches to depress MG levels in animal models may be  
133 beneficial, for example a recent study showing that AAV overexpression of Glo1, the  
134 enzyme that catalyzes MG, in endothelial cells improves function in a rat model of  
135 type 1 diabetes [13]. Unfortunately, approaches to reduce MG levels clinically have  
136 already failed. Specifically, compounds called “AGE-breakers”, drugs aimed at  
137 reducing levels of MG and AGE [14, 15] showed no benefit in clinical trials. In fact,  
138 one trial in patients with type 2 diabetes was terminated early due to a negative  
139 impact [16]. Our therapeutic strategy aims at correcting the dysfunction occurring at  
140 the myofilament level, since the myofilament is a highly tuneable system [17] that is  
141 likely amenable to this approach.

142 In this study, we show in diabetic human hearts without heart failure that MG  
143 modifications are already increased compared to non-diabetics and correlate with  
144 early myofilament dysfunction. A successful strategy for restoring function would  
145 need to be informed by first discovering the molecular mechanism(s) by which MG  
146 inhibited myofilament function. Therefore, we measured the impact of MG on  
147 myofilament kinetics, used a computer model of myofilament activation to predict  
148 molecular changes, and validated the predictions through biophysical assays. These  
149 comprehensive approaches revealed that MG decreases the rate constant for the  
150 transition of tropomyosin from its blocked state to its closed state on actin, effectively  
151 making it harder to activate the thin filament. The n-terminal domain of cardiac  
152 myosin binding protein C (cMyBPC) has been shown to activate the thin filament by  
153 altering tropomyosin’s position on actin [18]. Indeed, the effects of MG on  
154 myofilament calcium sensitivity were rescued by recombinant cMyBPC domains,  
155 suggesting that targeting thin filament activation could be a viable therapeutic  
156 strategy to break the connection between diabetes and heart failure.

157

158

## **Methods**

159

160 Expanded Methods are presented in Supplemental Material

161

### **Human and animal studies**

163 Human left ventricular tissue samples were obtained at the Medical University of

164 Graz from organ donors whose hearts were rejected for transplantation but did not

165 have heart failure. Human study protocols were approved by the Ethics Committee

166 at the Medical University of Graz (28-508 ex 15/16). All patients gave informed

167 consent and the investigation conformed to the principles outlined in the declaration

168 of Helsinki. Animal studies were approved by the Loyola University Chicago

169 Institutional Animal Care and Use Committee (IACUC number 2019029) according to

170 the NIH Guide for the Care and Use of Laboratory Animals. C57/Bl6J male mice 2-4

171 months of age were purchased from Jackson laboratories (Jackson labs, USA).

172 Animals were euthanised by placing them in an induction chamber with isoflurane

173 vaporizer (5%). The animal remained in the chamber until unconscious, as

174 determined by corneal reflex. Following isoflurane exposure, animals were

175 euthanised by cervical dislocation and heart extubating.

176

### **Mass spectrometry**

178 Myofilament samples were prepared as stated previously [4]. Samples were

179 run on a 4-12% SDS- PAGE gel, stained with Coomassie stain, actin and myosin

180 bands excised, and then de-stained overnight. Gel bands were prepared for mass

181 spectrometry by digesting them in 2 µg/band Trypsin/LysC protease mix (Thermo

182 Scientific) for 16 hours at 37 °C. 200 - 300 ng of peptides were loaded onto an

183 UltiMate 3000 nanoHPLC coupled to a LTQ Orbitrap XL (Thermo). MS data analysis

184 was performed using the Peaks Bioinformatics Software. For analysis, glycated

185 peptides were normalized to the corresponding total peptides for each sample.

186

### **Functional assessments and recombinant proteins**

188 Skinned myocytes were prepared as previously described [4, 19]. ATPase

189 activity and tension cost were measured in skinned fibers using an in-house system,

190 as previously [20, 21]. Cardiac myosin S1 and actin and tropomyosin were

191 expressed and purified as described in the Supplemental methods. Tropomyosin

192 blocked-to-closed state transition (KB) and ADP release were measured using  
193 stopped-flow methods [22] (see Supplementary methods for details).

194

#### 195 Computational modelling

196 A previously published model of myofilament Ca<sup>2+</sup> activation [24] was used to  
197 identify molecular changes to sarcomeric proteins that could plausibly explain  
198 observed effects of methylglyoxal on skinned cardiac fibres. Baseline parameters  
199 from the published model were used as a starting parameter set. The model was  
200 implemented and run in MATLAB (Mathworks) as previously described.

201

#### 202 Statistical analysis

203 Data are presented as mean ± standard error. Quantitative data were  
204 analysed using Prism 8 (GraphPad software) and stopped-flow data were analysed  
205 using MATLAB. All statistical analyses were performed using Student's t-test, paired  
206 Students t-test, chi-squared test, or two-way repeated measures ANOVA with Sidak  
207 post hoc test, depending on the data set, as indicated in the text. P<0.05 was  
208 considered significant.

209

210

## Results

### Diabetics have increased glycation that correlates with myofilament function

212 We previously showed that patients with diabetes and heart failure exhibited  
213 increased MG glycation of myofilament proteins, primarily actin and myosin [4]. Here,  
214 we first sought to measure these MG modifications in diabetics without heart failure,  
215 to test whether they might precede heart failure and represent a possible therapeutic  
216 target. We utilized left ventricular (LV) tissue from donor hearts without heart failure,  
217 and either with type II diabetes or without (Non-Diabetic,  $n = 9$ ; Diabetic,  $n = 6$ ,  
218 demographic and basic clinical data shown in **Table 1**).

219

220 Table 1. Human Subject Characteristics

	Non-Diabetic	Diabetic	P-value
n	9	6	
Age (years)	63 ± 7	61 ± 10	0.82
% Female	33	50	0.62
BMI	30 ± 7	29 ± 2	0.79
% Diabetes	0	100	0.0001
% Ischemia	0	0	N/A
LVEF (%)	66 ± 7	66 ± 4	0.92
% Hypertension	22	100	0.007
Anti-hypertensive drugs (%)	16	100	0.001
Oral anti-diabetics (%)	0	66	0.01
β blockers (%)	16	50	0.23

221 BMI, body mass index; LVEF, left ventricular ejection fraction. Statistics by Student's  
222 t-test or Chi-squared test.

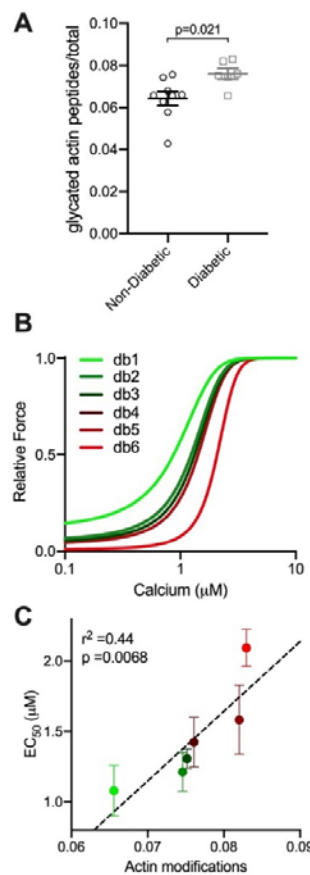
223

224 For each of these LV samples, the myofilament was enriched, separated by  
225 gel electrophoresis, and the actin and myosin bands excised and analysed for MG  
226 glycation by mass spectrometry. Diabetic patients exhibited significantly elevated  
227 glycation (including glyoxal and methylglyoxal-derived modifications) on sarcomeric  
228 actin compared to Non-Diabetic hearts (**Figure 1A, Supplemental Table 1**).  
229 However, no differences were observed in myosin glycation between the groups  
230 (**Supplemental Figure 1A, Supplemental Table 2**).

231 We next measured force-calcium relationships in skinned myocytes isolated  
232 from LV tissue from each Diabetic heart ( $n = 3 - 4$  myocytes per heart) to  
233 understand the impact of increased actin glycation on sarcomere function. For each  
234 Diabetic heart, the average fitted curve for all myocytes measured from that heart



235 are shown in **Figure 1B**, from the heart exhibiting the lowest level of actin glycation  
236 (db1, green line) to the highest level (db6, red line). A progressive rightward shift in  
237 the force-calcium relationship (calcium desensitization) was observed with increasing  
238 levels of actin glycation. This correlation was confirmed when mean calcium  
239 sensitivity of all cardiomyocytes from each subject was plotted against the level of  
240 actin glycation for each subject (**Figure 1C**). The strong positive correlation ( $r^2 =$   
241 0.44,  $p = 0.0068$  for a non-zero slope by linear regression), indicates that in diabetic  
242 hearts, increased levels of actin glycation are associated with a progressive  
243 decrease in myofilament calcium sensitivity (increased  $EC_{50}$ ).



244 **Figure 1: Glycation of sarcomeric actin was increased in Diabetic**  
245 **compared to Non-Diabetic subjects and correlates with decreased myofilament**  
246 **calcium sensitivity.** (A) Glycated peptides normalized to total peptides as  
247 measured by mass spectrometry on actin, from Non-Diabetic (black circles,  $n=9$ ) and  
248 Diabetic (grey squares,  $n=6$ ) left ventricular tissue. Statistical comparison by  
249 Student's t-test. (B) Mean fitted curves for force as a function of calcium  
250 concentration in human skinned myocytes isolated from Diabetic subjects ( $n=3-4$   
251 myocytes per subject,  $n=6$  subjects) for the subject with the lowest (db1, green) to  
252 highest level of actin glycation (db6, red), showing progressive desensitization to  
253 calcium in subjects with increased glycation. (C) Mean  $EC_{50}$  as a function of total  
254 actin glycation detected by mass spectrometry for each human Diabetic sample  
255

256 (circles colour coded from the lowest glycation level, bright green to highest glycation  
257 level, bright red,  $n=6$ ). The data are described by a positive correlation (dashed line,  
258  $r^2=0.44$ ,  $p= 0.0068$  by linear regression.  
259

260 Not all diabetic patients eventually develop heart failure, however. Indeed,  
261 while we observed increased actin glycation overall, some subjects had levels equal  
262 to Non-Diabetics. As such, some subjects exhibited normal myofilament function, so  
263 that no overall differences were observed in maximal calcium-activated force ( $F_{max}$ )  
264 or calcium sensitivity ( $EC_{50}$ ) between Non-Diabetic versus Diabetic samples  
265 (**Supplemental Figure 1B-D**). Myofilament calcium desensitization does not always  
266 result in concurrent observable global dysfunction [23], but is known to be  
267 pathogenic for dilated cardiomyopathy and heart failure. Thus, in diabetics with  
268 increased glycation, MG modifications represent a possible therapeutic target to  
269 reduce the risk of developing heart failure in the progression of diabetic  
270 cardiomyopathy.

271

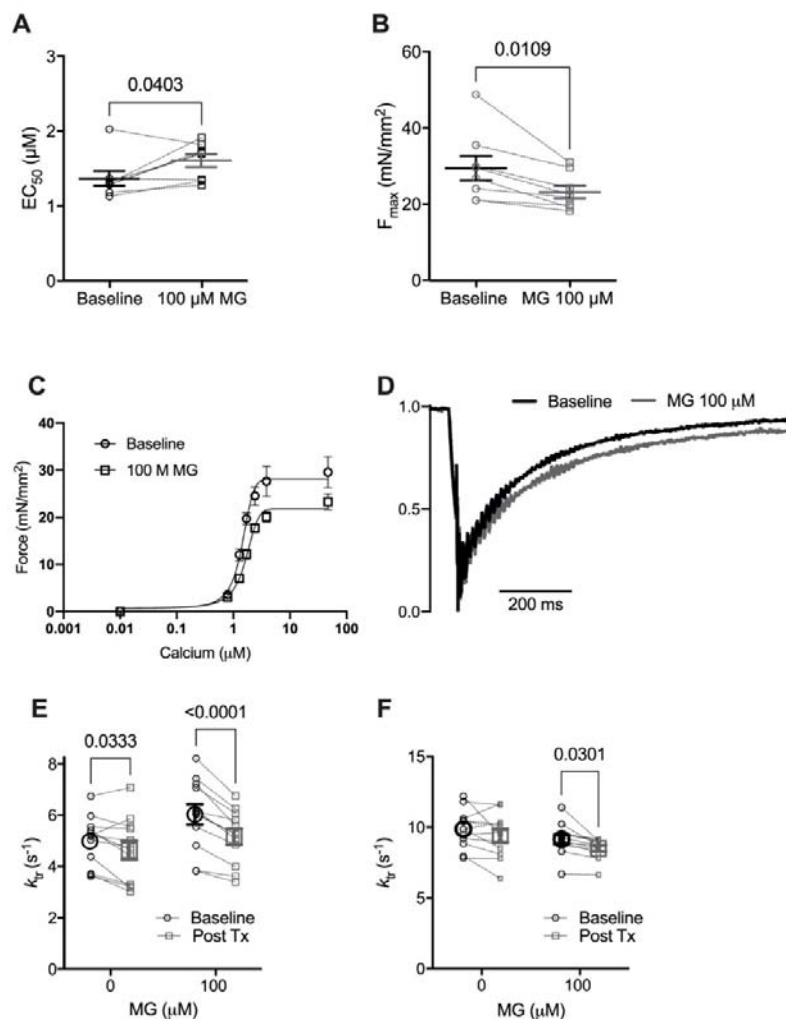
#### 272 Computational predications of molecular processes dysregulated by MG

273 Our next goal was to determine the molecular mechanism(s) of action of MG,  
274 as myofilament functional parameters like calcium sensitivity are an aggregate  
275 measurement of numerous molecular processes [24]. To predict which of these  
276 processes are modified by MG we used a multiscale computer model of cooperative  
277 myofilament activation [25]. To adequately constrain the model, it is necessary to  
278 know the functional impact of MG on both steady-state and kinetic parameters.

279 To measure these parameters, we used skinned myocytes isolated from LV  
280 tissue from three-month-old male C57Bl6/j mice treated with 100  $\mu$ M MG for 20  
281 mins. In healthy tissue, levels of free MG are around 1 – 10  $\mu$ M [6, 26, 27] and  
282 approximately double in disease [28]. However, the majority of MG is found on  
283 glycated proteins [29], meaning these measurements of free MG significantly under-  
284 estimate the amount of MG glycation that occurs. To ensure this MG treatment  
285 increased glycation of the myofilament, we treated mouse left ventricular skinned  
286 myocytes with 100  $\mu$ M MG for 20 mins. We then solubilized these samples, ran them  
287 on SDS PAGE gels, excised actin and myosin bands, and analysed them via high  
288 resolution nHPLC-MS/MS. We found that MG modifications on actin and myosin

289 were increased after the *in vitro* MG treatment (**Supplemental Figure 2 and**  
290 **Supplementary Table 3, 4**).

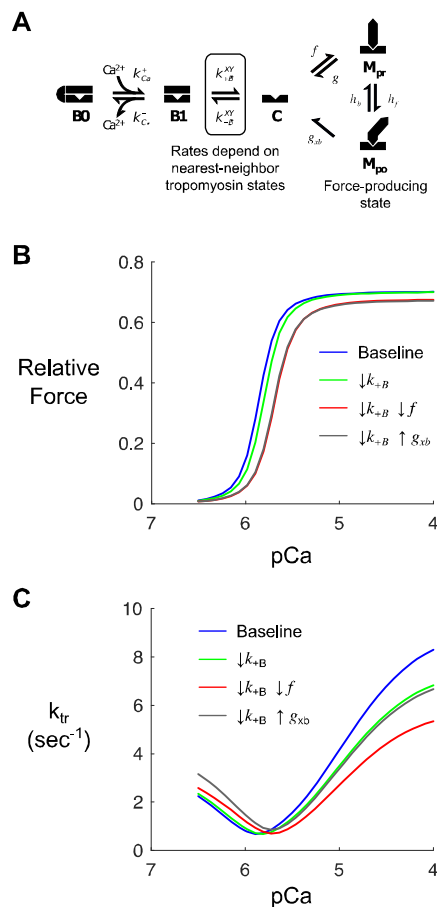
291 The impact of MG on steady-state parameters is described by the force-  
292 calcium relationship. As we had shown previously [4], exposure to MG decreased  
293 both calcium sensitivity and  $F_{\max}$  (**Figure 2A-C**). To determine the effect on kinetics,  
294 we measured the rate of force recovery after a slack-restretch maneuver ( $k_{tr}$ ) before  
295 and after MG treatment. Further,  $k_{tr}$  was measured when the myocyte was exposed  
296 to either maximal (46.8  $\mu\text{M}$ ) or submaximal (1.7058  $\mu\text{M}$ , approximately  $\text{EC}_{50}$ )  
297 calcium. Treatment with 100  $\mu\text{M}$  MG decreased  $k_{tr}$  at maximal and sub-maximum  
298  $\text{Ca}^{2+}$  activation (**Figure 2D-F**).



299  
300 **Figure 2: Methyglyoxal decreases calcium sensitivity, maximal calcium-**  
301 **activated force and rate of force redevelopment ( $k_{tr}$ ).** (A) Individual and mean  $\pm$   
302 SEM calculated  $\text{EC}_{50}$  (panel A) and  $F_{\max}$  (panel B). (C) Mean force as a function of  
303 calcium concentration and fitted curves for mouse skinned myocytes before (circles,  
304 solid line) and after (squares, dashed line) exposure to 100  $\mu\text{M}$  Methylglyoxal (MG).

305 (D) Normalized  $k_{tr}$  curve before (black) and after (grey) treatment with 100  $\mu\text{M}$  MG at  
 306 submaximal  $\text{Ca}^{2+}$  concentration (average from 12 cells). (E) Individual and mean  $\pm$   
 307 SEM calculated  $k_{tr}$  values before (Baseline, black circles) or after (Post Tx, grey  
 308 squares) treatment with 0 (no treatment) or 100  $\mu\text{M}$  MG at sub-maximal  $\text{Ca}^{2+}$   
 309 concentration ( $n=12$  myocytes from 4 mice,  $p_{\text{interaction}} = 0.016$ ) (Mean  $\pm$  SEM). (F)  $k_{tr}$   
 310 before (black circles) or after (grey squares) treatment with 0 or 100  $\mu\text{M}$  MG at  
 311 maximal  $\text{Ca}^{2+}$  concentration ( $n=12$  myocytes from 4 mice,  $p_{\text{interaction}} = \text{n.s.}$ ). Statistical  
 312 comparisons made with 2-way repeated measures ANOVA with Sidak post-hoc test.  
 313

314 Next, using the computational model of myofilament activation, individual model  
 315 parameters were adjusted in an attempt to recapitulate the differences between the  
 316 baseline and MG-treated functional data (Figure 3A). The model was first used to  
 317 generate baseline force-calcium (blue line, Figure 3B) and  $k_{tr}$ -calcium (blue line,  
 318 Figure 3C) relationships, using previously published baseline model parameters  
 319 [25]. We then altered individual or combinations of parameters to recapitulate the  
 320 simultaneous impact on  $\text{EC}_{50}$  (Figure 2A),  $F_{\text{max}}$  (Figure 2B) and  $k_{tr}$  (Figure 2D-F).



321  
 322  
 323  
 324

**Figure 3: Computer modelling to identify potential methylglyoxal molecular effects.** (A) Kinetic scheme for a previously published model of myofilament  $\text{Ca}^{2+}$  activation [24]. The model depicts states of thin filament regulatory

325 units (B0, blocked and  $\text{Ca}^{2+}$ -free; B1, blocked and  $\text{Ca}^{2+}$ -bound; C, closed) and  
326 cycling of associated myosin crossbridges ( $M_{\text{pr}}$ , myosin pre-powerstroke;  $M_{\text{po}}$ ,  
327 myosin post-powerstroke). **(B)** Steady-state force-pCa curves produced by the  
328 model under baseline (control) conditions and various perturbations intended to  
329 qualitatively mimic observed effects of MG. Simulations show the anticipated effects  
330 of slowing the blocked-closed transition of tropomyosin ( $k_{+B}$ ) on its own (green) or in  
331 combination with slowing myosin attachment ( $f$ , red) or myosin detachment ( $g$ , gray).  
332 **(C)** Model-predicted  $k_{\text{tr}}$ -pCa relationships corresponding to the same conditions as in  
333 panel B.

334

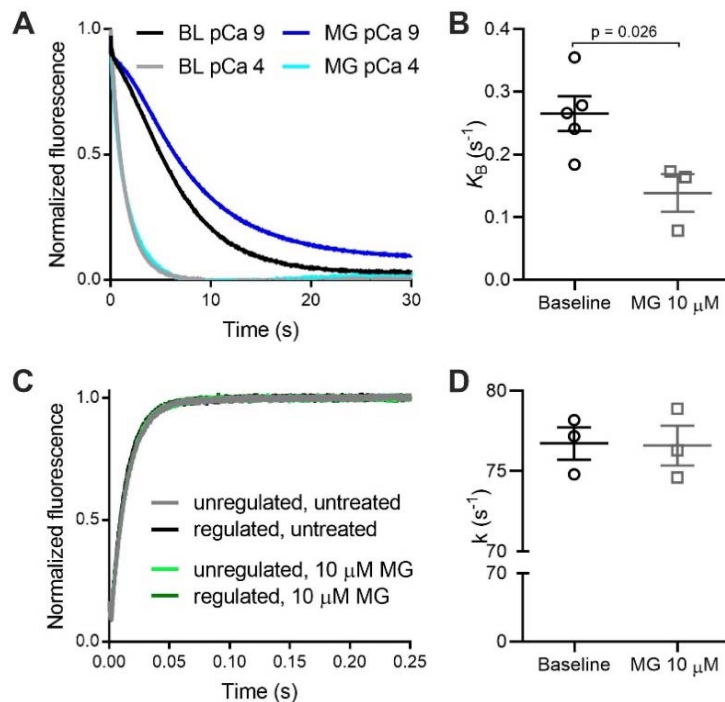
335 The model indicated that simultaneous changes in two parameters were  
336 sufficient to reproduce this behaviour: 1) a ~10% decrease in the tropomyosin  
337 blocked-to-closed rate transition ( $K_B$ ) and 2) a decrease in the myosin crossbridge  
338 duty cycle from either a 20% decrease in the myosin binding rate ( $f$ ) or a 30%  
339 increase in the myosin detachment rate ( $g_{\text{xb}}$ ). The individual and combined effects of  
340 these changes are shown in green, red, and grey on **Figure 3 B, C**. We  
341 subsequently searched for experimental evidence that MG treatment affected these  
342 molecular processes.

343

#### 344 MG increases the probability of thin filaments being in the “blocked” state

345 Tropomyosin is found in three positions on actin: blocked, closed and open.  
346 These positions are determined by calcium and myosin binding to the thin filament  
347 [30-32]. The equilibrium constant describing the transition from the blocked to closed  
348 tropomyosin state ( $K_B$ ) was determined using stop flow experiments, where the rate  
349 of myosin binding to pyrene-labelled regulated thin filaments was measured at high  
350 (pCa 4) and low (pCa 9) calcium concentrations [22, 32]. The observed rates for  
351 myosin S1 binding to the thin filament at high and low calcium were used to calculate  
352 the equilibrium constant,  $K_B$  (see Supporting Materials for details). Since these  
353 experiments have not been previously performed, we needed to examine the effects  
354 on both the lower and the higher dose of MG on thin filaments. Stopped-flow  
355 experiments were performed using reconstituted regulated thin filaments before and  
356 after exposure to 10  $\mu\text{M}$  MG for 20 mins. MG decreased  $K_B$  by approximately 50% in  
357 regulated thin filaments (**Figure 4A, B**). A decreased equilibrium constant means  
358 that the blocked state will be more favoured over the closed state. Although we  
359 cannot exclude the possibility that MG decreases  $K_B$  by increasing the rate of the

360 closed-to-blocked transition, the decrease in  $K_B$  is consistent with the reduced rate of  
 361 the blocked-to-closed transition predicted by the computational modelling.



362

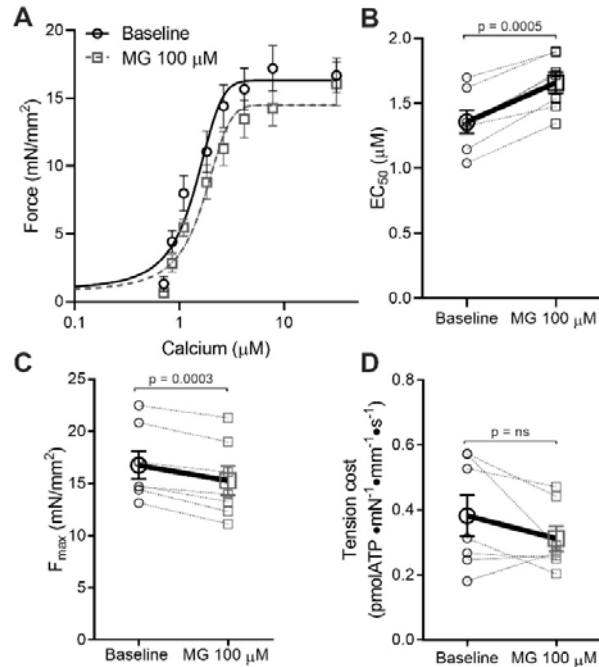
363 **Figure 4: Methyglyoxal decreases the tropomyosin blocked-to-closed rate**  
 364 **transition.** (A) Normalized fluorescence of pyrene-labelled actin as myosin S1 binds  
 365 to regulated thin filaments at pCa 4 (high calcium) and pCa 9 (low calcium). The  
 366 pyrene fluorescence decreases upon S1 binding. Rate of myosin S1 binding to  
 367 regulated thin filaments is higher at pCa 4 due to thin filament activation by calcium.  
 368 The difference in the rates at pCa 4 and pCa 9 is used to calculate  $K_B$ . The black and  
 369 grey lines represent untreated filaments (BL) and the dark/light blue lines represent  
 370 thin filaments treated with 10  $\mu$ M MG. (B) Individual and mean  $\pm$  SEM  $K_B$  values for  
 371 untreated (baseline, black dots,  $n=5$ ) or treated thin filaments with 10  $\mu$ M MG (grey  
 372 squares,  $n=3$ ). (C) Measurement of the actomyosin detachment rate. Normalized  
 373 fluorescence of pyrene-labelled actin as myosin S1 bound to ADP detaches from  
 374 regulated thin filaments upon addition of ATP. The rate of actomyosin detachment is  
 375 measured from the increase in pyrene fluorescence. Unregulated filaments (black,  
 376 grey) or regulated filaments (dark/light green) treated or not with 10  $\mu$ M MG. (D)  
 377 Individual and mean  $\pm$  SEM rate constant ( $k$ ) for ADP release from myosin S1  
 378 binding to regulated thin filaments untreated (baseline, black circles) or treated with  
 379 10  $\mu$ M MG (grey squares) ( $n=3$  for each). Statistical comparisons by Students t-test.  
 380

381 The model also predicted MG either increases the crossbridge detachment  
 382 rate or decreases the attachment rate. By stopped-flow, we can measure the  
 383 detachment rate constant ( $k$ ) of ADP release from actomyosin solution, which is the  
 384 transition that limits crossbridge detachment rate at physiological ATP

385 concentrations. We performed stopped-flow experiments by rapidly mixing 1)  
386 pyrene-labelled thin filaments pre-incubated with myosin S1 and ADP with 2)  
387 solution containing saturating ATP [33]. When thin filaments were incubated with 10  
388  $\mu\text{M}$  MG for 20 mins there was no difference in ADP release (**Figure 4C, D**). Even at  
389 the higher 100  $\mu\text{M}$  dose, MG had no effect on the crossbridge detachment rate  
390 measured using reconstituted proteins in solution (**Supplemental Figure 3**).

391 To confirm the biochemical stopped-flow results in a more physiological  
392 system, we measured ATPase activity and active force production simultaneously in  
393 skinned mouse papillary fibers. Tension cost (the ratio of myosin ATPase activity to  
394 force production) is directly proportional to the number of post-power stroke  
395 crossbridges and therefore represents a measurement of the crossbridge  
396 detachment rate. We found that 40 mins incubation with MG decreased calcium  
397 sensitivity and  $F_{\text{max}}$ , (as in skinned myocytes) as well as ATPase activity (**Figure 5**).  
398 The longer incubation time (40 minutes vs 20 minutes in skinned cells) was  
399 necessary because of the larger size of the fiber bundles. Since MG decreased both  
400 force and ATPase activity in parallel, there was no effect on tension cost (the  
401 ATPase activity to Force ratio), indicating that MG has no effect on the crossbridge  
402 detachment rate. By two measurements we confirm that MG has no effect on the  
403 crossbridge detachment rate, suggesting MG decreases the crossbridge attachment  
404 rate.





405  
406  
407  
408  
409  
410  
411  
412  
413  
414  
415

**Figure 5: Methyglyoxal does not alter tension cost of mouse skinned fibers.**

(A) Average force-calcium data and fitted curves for skinned fibers before (black circles, solid line) or after (grey squares, dashed line) treatment with 100 μM MG for 40 mins ( $n=7$  fibers from 4 mice). (B) Individual and mean  $\pm$  SEM calculated EC<sub>50</sub> values before (baseline, black circles) or after 100 μM MG (grey squares). (C) F<sub>max</sub> before (baseline, black circles) or after 100 μM MG (grey squares) ( $n=7$  fibers from 4 different mice). (D) Tension cost was calculated via the ratio of ATPase activity over force, before (baseline, black circles) or after 100 μM MG (grey squares). Statistical comparisons made by student's paired t-test.

416 N-terminal MyBPC fragment rescues MG-induced dysfunction but OM does not.

417 Having established that MG depresses myofilament function by inhibiting  
418 tropomyosin movement on actin, we next aimed to determine whether we could  
419 rescue calcium sensitivity by specifically targeting these mechanisms. However, we  
420 first wanted to confirm that reducing MG itself is not an effective therapy. We used  
421 aminoguanidine (AG), an agent that has been reported to scavenge MG and prevent  
422 it from forming further modifications [34]. Skinned myocytes were pre-treated with  
423 100 μM MG for 20 mins, a force-calcium relationship was measured, then treated  
424 with 1 mM AG for 5 mins and a second force-calcium relationship measured. This  
425 dose of AG and treatment time was chosen because previous experiments in intact  
426 isolated cardiomyocytes showed it was capable of improving function [35]. However,  
427 we found that AG had no effect on calcium sensitivity or F<sub>max</sub> (**Supplemental Figure**  
428 **4**), indicating it was unable to reverse the deleterious functional effects of MG.

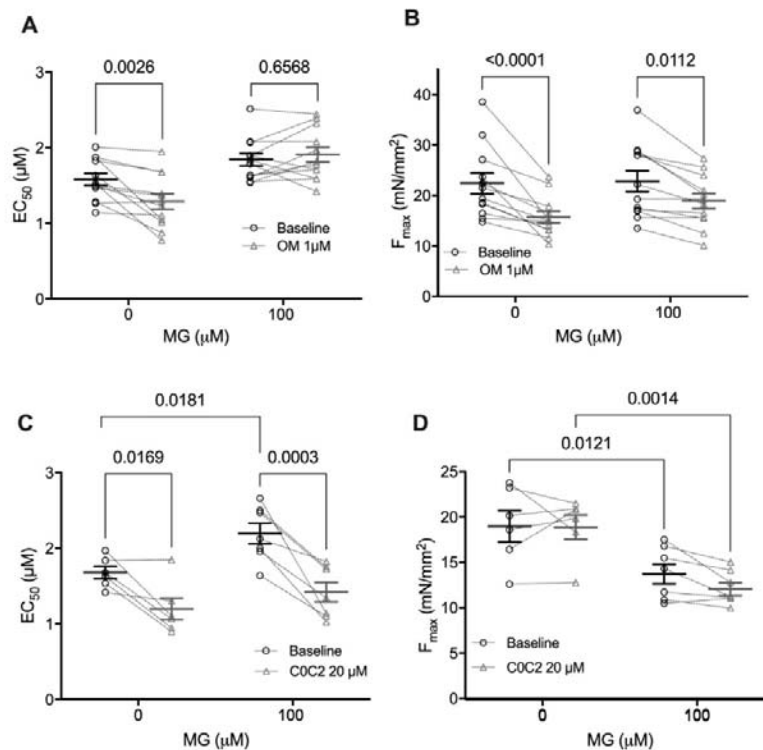


429           Next, we supposed that calcium sensitizers that did not target tropomyosin  
430 might be ineffective at rescuing MG-induced dysfunction. Thus, we first used  
431 Omecamtiv Mecarbil (OM), a myosin activator which increases  $Ca^{2+}$  sensitivity in  
432 isolated cardiomyocytes [36]. We hypothesized that MG's impact on tropomyosin  
433 would block the OM-activated myosin heads from binding actin, and thus not be  
434 rescued with this treatment. We found that in the absence of MG, treatment with 1  
435  $\mu$ M OM for 2 mins increased calcium sensitivity and decreased  $F_{max}$  as previously  
436 [36]. However, in skinned myocytes pre-incubated with 100  $\mu$ M MG for 20 mins, OM  
437 had no effect on  $Ca^{2+}$  sensitivity and further reduced  $F_{max}$  (**Figure 6A,B**). These  
438 results indicate that OM is not effective in reversing the functional defects by MG,  
439 possibly even exacerbating the dysfunction by further reducing  $F_{max}$ , supporting  
440 MG's action through tropomyosin.

441           Knowing that MG increases the population of thin filaments in the inhibitory  
442 blocked state, we next aimed to discover whether a molecule that activates the thin  
443 filament could reverse the action of MG on the sarcomere. Currently, there are no  
444 small molecules that act on tropomyosin [37-39], so we used recombinant cMyBPC  
445 C0C2 peptide, which has been shown to activate the thin filament by pushing  
446 tropomyosin into positions that are more permissive for myosin binding to the thin  
447 filament [40]. The cMyBPC C0C2 peptide consists of the 466 n-terminal amino acids  
448 that encompass the cardiac specific C0 domain, two Ig domains (C1, C2), a proline-  
449 alanine linker between C1 and C2, and a unique cMyBPC "motif" or M-domain that  
450 connects C1 and C2. We hypothesized that C0C2 would be able to reverse the  
451 functional defects of MG through likewise displacing tropomyosin.

452           In mouse skinned myocytes not exposed to MG, incubation with 20  $\mu$ M C0C2  
453 for 20 minutes increased calcium sensitivity with no change in  $F_{max}$  (**Figure 6C, D**),  
454 which is in line with published data [41, 42]. At this concentration of C0C2, it is  
455 known to interact with actin [42, 43] and is thus likely to impact tropomyosin's  
456 position on actin as intended. Skinned myocytes pre-incubated with 100  $\mu$ M MG  
457 were significantly desensitized to calcium ( $p = 0.036$  by two-way ANOVA) and  
458 trended towards a decrease in  $F_{max}$  ( $p = 0.052$  by two-way ANOVA), recapitulating  
459 our prior data. When these MG-preincubated myocytes were treated with C0C2 for  
460 20 minutes,  $Ca^{2+}$  sensitivity was restored (from  $EC_{50} = 2.19$  to 1.42,  $p = 0.0018$  by two-  
461 way ANOVA,  $n = 7$ , **Figure 6C**). While there was a significant decrease in  $F_{max}$  with

462 C0C2 treatment in the MG-exposed myocytes (from  $F_{max} = 13.9$  to  $12.2$ ,  $p=0.043$  by  
463 two-way ANOVA,  $n = 7$ , **Figure 6D**), the magnitude of this decrease was less than  
464 15% of the pre-treatment level and is likely due to normal myocyte rundown during  
465 multiple activations. Furthermore, there was no interaction between C0C2 and MG  
466 treatments on the effect of  $F_{max}$  ( $p = 0.57$  by two-way ANOVA). Overall, these data  
467 show that C0C2 can reverse the depressed calcium sensitivity caused by MG,  
468 presumably by moving tropomyosin on actin into a position that is favourable for  
469 myosin contraction.



470

471 **Figure 6: C0C2 rescues the calcium sensitivity decrease caused by MG in**  
472 **skinned cardiomyocytes but OM does not.** (A) Individual and mean  $\pm$  SEM  $EC_{50}$   
473 values from skinned myocytes pre-exposed to 0  $\mu M$  MG ( $n=6$ ) or 100  $\mu M$  MG ( $n=7$   
474 from 3-4 mice) before treatment with cardiac myosin binding protein C peptide C0C2  
475 (baseline, black circles) or after (C0C2 20  $\mu M$ , grey triangles). Paired before and  
476 after data for an individual cell are connected by dashed lines. (B) Individual and  
477 mean  $\pm$  SEM  $F_{max}$  values from skinned myocytes pre-exposed with 0  $\mu M$  MG ( $n=4$ )  
478 or 100  $\mu M$  MG ( $n=7$  from 3 mice) before with C0C2 (baseline, black circles) or after  
479 (C0C2 20  $\mu M$ , grey triangles). Individual and mean  $\pm$  SEM calculated  $EC_{50}$  (panel G)  
480 and  $F_{max}$  (panel F) from skinned myocytes pre-exposed to 0  $\mu M$  MG ( $n=8$ ) or 100  $\mu M$   
481 MG ( $n= 12$  from 4 mice) before (baseline, black circles) or after treatment with 1  $\mu M$   
482 Omecamtiv Mecarbil (1  $\mu M$  OM, grey triangles) ( $n=12$  myocytes from 4 mice). Paired  
483 before and after treatment data for each individual cell are connected by dashed  
484 lines. Statistical comparisons by two-way repeated measures ANOVA with Sidak  
485 post-hoc test.

486

## Discussion

487

488 We have shown for the first time that diabetics free of heart failure exhibit  
489 increased MG actin glycation compared to those without diabetes. In diabetics, the  
490 magnitude of elevated glycation positively correlated with myofilament  
491 desensitization to calcium. Not all diabetics eventually develop heart failure, so it is  
492 reasonable that in this cohort we would detect a range of glycation and function. It is  
493 thus unlikely that overt dysfunction could be used to predict the eventual  
494 development of heart failure in diabetics, and MG modifications may represent a  
495 more sensitive biomarker. We hypothesize those subjects with high levels of  
496 glycation and calcium desensitization would be the most likely to develop diabetic  
497 cardiomyopathy and heart failure [2]. As these were donor hearts, it is impossible to  
498 know for sure whether they would have eventually developed cardiac dysfunction,  
499 however, point mutations that cause familial dilated cardiomyopathy frequently cause  
500 similar myofilament calcium desensitization that eventually leads to heart failure [12].  
501 Thus, the cellular dysfunction induced by this glycation represents a possible  
502 therapeutic target for inhibiting the development of diabetic cardiomyopathy [44],  
503 which can lead to heart failure [45].

503

504 In non-failing diabetics, the median magnitude of the increase in actin  
505 glycation was about half of what we previously observed in diabetic patients with  
506 heart failure (~20% vs ~40% increase compared to controls [4]). This relationship  
507 suggests that myofilament MG glycation increases in parallel with disease severity,  
508 preceding global cardiac dysfunction. Importantly, while our previous work was in  
509 diabetic heart failure patients [4], these findings in otherwise healthy diabetics  
510 decouple the impact of myofilament glycation on cardiomyocyte function from  
511 adaptive and maladaptive processes occurring during end-stage heart failure. That  
512 the increased glycation was detected only on actin, and not myosin, was unexpected  
513 but suggests a preference for MG glycation. While no previous studies have  
514 identified any site specificity for MG glycation, these data indicate there are certainly  
515 preferred targets, possibly due to length or concentration of MG exposure as well as  
516 the accessibility and reactivity of the modified residues. The increased levels of MG  
517 glycation on solely actin are still harmful as our previous work showed dysfunction  
518 was induced by MG glycation of actin or myosin independently [4].

518

519 Unfortunately, broadly targeting the MG-induced dysfunction with compounds  
520 that inhibit MG modifications or general systolic activators was unsuccessful in

520 reversing the dysfunction. A combination of biophysical functional approaches,  
521 computer simulation, and stopped-flow experiments revealed that MG modifications  
522 increase the population of the tropomyosin blocked state, therefore inhibiting myosin  
523 from binding to the thin filament and initiating contraction. Effectively, MG makes it  
524 more difficult to activate the thin filaments to allow force production. By targeting this  
525 mechanism specifically, using a thin-filament interacting peptide of myosin binding  
526 protein C, we were thus able to rescue MG-induced calcium desensitization.

527 Our previously published mass spectrometry data provides a possible  
528 mechanism for how MG affects tropomyosin movement. We found MG glycation of  
529 actin K291 [4], which is within a critical region of actin termed the “A-triad”, a cluster  
530 which stabilizes the A-state structure, which is similar to the blocked state [46].  
531 Mutations and modifications to residues in this region have been shown to alter  
532 function by either stabilizing or de-stabilizing the A-state [47]. We propose that MG  
533 forms an irreversible glycation modification on K291 residue in the A-triad, changing  
534 the allosteric interactions between actin and tropomyosin to stabilize the blocked  
535 state of tropomyosin and therefore reduce  $K_B$  and myofilament calcium sensitivity  
536 **(Supplemental Figure 5)**.

537 The computer model also predicted MG glycation inhibits the crossbridge duty  
538 cycle, although the model is unable to differentiate between either a decrease in  $f$   
539 (crossbridge attachment rate) or an increase in  $g$  (crossbridge detachment rate). The  
540 stopped flow and tension cost data both indicated that the detachment rate was  
541 unchanged. Combined with the model, these data highly suggest that MG decreases  
542 the crossbridge attachment rate. Unfortunately, measuring the attachment rate  
543 requires proteins in saturated conditions (i.e., non-physiological), and is challenging  
544 to measure with rigorous approaches, so this cannot be confirmed at present.  
545 However, one possible explanation for how MG could decrease the attachment rate  
546 is by affecting the super-relaxed state of myosin [48]. If MG enhances the super-  
547 relaxed state and fewer myosin heads are available to form crossbridges, this could  
548 appear as a reduced rate of attachment ( $f$ ). The stopped-flow experiments do not  
549 include the impact of the super-relaxed state, so it is not possible to account for its  
550 effect. Furthermore, while the tension cost experiments presumably do include the  
551 super-relaxed state, myosin heads in this state have a very low basal ATPase  
552 activity [49] and might have little effect on the measured tension cost. Thus, whether

553 MG alters the super-relaxed state remains an unaccounted-for possibility in this  
554 study.

555 Our results in myocytes not exposed to MG agree with prior studies showing  
556 OM increases myofilament calcium sensitivity [36] and reduces  $F_{max}$  likely by  
557 depressing the myosin working stroke [50]. We showed that MG blocked the calcium  
558 sensitizing effect of OM but did not affect its ability to decrease  $F_{max}$ , indicating that  
559 MG causes OM to act as a negative inotrope. Our finding that MG keeps  
560 tropomyosin in the “blocked” position can mechanistically explain this effect. First,  
561 OM primes myosin heads to increase their binding to actin to form force-generating  
562 crossbridges at submaximal calcium [51], but since MG inhibits thin filament  
563 activation, this calcium sensitizing effect is blocked. Furthermore, OM decreases  
564  $F_{max}$  by decreasing the myosin working stroke, which would be unaffected by  
565 tropomyosin positioning.

566 Finally, the C0C2 domains of cMyBPC were able to restore the MG-induced  
567 decrease in calcium sensitivity. The mechanism of C0C2’s benefit is likely by  
568 counteracting the MG-induced reduction in tropomyosin’s blocked-to-closed  
569 transition rate, as it has been suggested that C0C2 can alter tropomyosin’s position  
570 on actin [18, 52]. These findings provide a strong proof-of-principle that specifically  
571 targeting the molecular mechanism of MG can rescue function. However, the C0C2  
572 peptide was not able to restore the decrease in  $F_{max}$  caused by MG. The inability of  
573 C0C2 to restore  $F_{max}$  supports the model prediction that there are two separate  
574 effects of MG glycation on the sarcomere, and C0C2 only affects one of these.  
575 Whether this second effect is a decrease in the crossbridge attachment rate as the  
576 model and experiments suggest and if this dysfunction can likewise be reversed will  
577 have to be determined in future studies. Furthermore, whether the C0C2 cMyBPC  
578 fragment could be an appropriate therapeutic option in the clinic is not clear. The  
579 C0C2 peptide contains the regulatory region of cMyBPC that includes  
580 phosphorylation sites that are important for the sarcomere’s response adrenergic  
581 stimulation [43, 53, 54], so the peptide would be susceptible to modulation by  
582 phosphorylation *in vivo*. However, a recent study expressed the C0C2 peptide using  
583 AAV, and showed it was capable of rescuing function in a cMyBPC knockout mouse  
584 [55], suggesting the peptide is stable and functional *in vivo*.

585

586

## Conclusion

587 Overall, this study provides a proof of principal that either C0C2 or another  
588 therapeutic that can move tropomyosin towards the “open” state would be a potential  
589 therapeutic avenue for patients who have diabetes and either have heart failure or  
590 are at risk of developing it. As initial treatment approaches failed, such as AGE-  
591 breakers, it was critical that we identified this specific mechanism of MG glycation  
592 using biophysical, computational, and chemical kinetics. Furthermore, as no small  
593 molecules currently target tropomyosin, these results provide rationale that future  
594 drug discovery efforts should explore this mechanism. These insights provide a  
595 strong foundation for future work targeting these mechanisms to stem the increase in  
596 heart failure cases that will occur as the prevalence of diabetes continues to grow  
597 worldwide.

598

599 **Funding:** This work was funded by the American Heart Association  
600 (111POST7210031 to M.P.), the National Institutes of Health (R01HL136737 to  
601 J.A.K. and R01HL 141086 to M.J.G), the Children’s Discovery Institute of  
602 Washington University and St. Louis Children’s Hospital (PM-LI-2019-829 to M.J.G.),  
603 the Austrian Science Fund (I 4168-B to P.P.R.), and the European Research Area  
604 Network (ERA-CVD to P.P.R.).

605

606 **Author contribution:** M.P. and J.A.K. designed the project and research studies.  
607 M.P., T.K., S.K.B. and S.G.C. conducted experiments and acquired data. M.P.,  
608 S.K.B., S.C.G., M.J.G. and J.A.K. interpreted experimental results. M.P., S.G.C. and  
609 J.A.K. analysed data and created figures. P.P.R., D.L. and S.P.H. provided peptide  
610 and human samples. M.P. and J.A.K. wrote the manuscript. T.K., S.K.B., S.G.C.,  
611 D.L., P.P.R., S.P.H. and M.J.G. revised the manuscript.

612

613 **Conflict of Interest:** None declared



614

615

## References

- 616 1. Saeedi, P., et al., *Global and regional diabetes prevalence estimates for 2019*  
617 *and projections for 2030 and 2045: Results from the International Diabetes*  
618 *Federation Diabetes Atlas, 9(th) edition*. Diabetes Res Clin Pract, 2019. **157**:  
619 p. 107843.
- 620 2. Kenny, H.C. and E.D. Abel, *Heart Failure in Type 2 Diabetes Mellitus*. Circ  
621 Res, 2019. **124**(1): p. 121-141.
- 622 3. Dei Cas, A., et al., *Impact of diabetes on epidemiology, treatment, and*  
623 *outcomes of patients with heart failure*. JACC Heart Fail, 2015. **3**(2): p. 136-  
624 45.
- 625 4. Papadaki, M., et al., *Diabetes with heart failure increases methylglyoxal*  
626 *modifications in the sarcomere, which inhibit function*. JCI Insight, 2018. **3**(20).
- 627 5. Phillips, S.A. and P.J. Thornalley, *The formation of methylglyoxal from triose*  
628 *phosphates. Investigation using a specific assay for methylglyoxal*. Eur J  
629 Biochem, 1993. **212**(1): p. 101-5.
- 630 6. Rabbani, N. and P.J. Thornalley, *Methylglyoxal, glyoxalase 1 and the*  
631 *dicarbonyl proteome*. Amino Acids, 2012. **42**(4): p. 1133-42.
- 632 7. Hegab, Z., et al., *Role of advanced glycation end products in cardiovascular*  
633 *disease*. World J Cardiol, 2012. **4**(4): p. 90-102.
- 634 8. Soman, S., et al., *A multicellular signal transduction network of AGE/RAGE*  
635 *signaling*. J Cell Commun Signal, 2013. **7**(1): p. 19-23.
- 636 9. Schalkwijk, C.G. and C.D.A. Stehouwer, *Methylglyoxal, a Highly Reactive*  
637 *Dicarbonyl Compound, in Diabetes, Its Vascular Complications, and Other*  
638 *Age-Related Diseases*. Physiol Rev, 2020. **100**(1): p. 407-461.
- 639 10. Shao, C.H., et al., *Carbonylation contributes to SERCA2a activity loss and*  
640 *diastolic dysfunction in a rat model of type 1 diabetes*. Diabetes, 2011. **60**(3):  
641 p. 947-59.
- 642 11. Shao, C.H., et al., *Carbonylation induces heterogeneity in cardiac ryanodine*  
643 *receptor function in diabetes mellitus*. Mol Pharmacol, 2012. **82**(3): p. 383-99.
- 644 12. Du, C.K., et al., *Knock-in mouse model of dilated cardiomyopathy caused by*  
645 *troponin mutation*. Circ Res, 2007. **101**(2): p. 185-94.
- 646 13. Alomar, F.A., et al., *Adeno-Associated Viral Transfer of Glyoxalase-1 Blunts*  
647 *Carbonyl and Oxidative Stresses in Hearts of Type 1 Diabetic Rats*.  
648 *Antioxidants (Basel)*, 2020. **9**(7).
- 649 14. Moreau, R., et al., *Reversal by aminoguanidine of the age-related increase in*  
650 *glycooxidation and lipoxidation in the cardiovascular system of Fischer 344*  
651 *rats*. Biochem Pharmacol, 2005. **69**(1): p. 29-40.
- 652 15. Dhar, A., et al., *Alagebrium attenuates methylglyoxal induced oxidative stress*  
653 *and AGE formation in H9C2 cardiac myocytes*. Life Sci, 2016. **146**: p. 8-14.
- 654 16. Engelen, L., C.D. Stehouwer, and C.G. Schalkwijk, *Current therapeutic*  
655 *interventions in the glycation pathway: evidence from clinical studies*.  
656 *Diabetes Obes Metab*, 2013. **15**(8): p. 677-89.
- 657 17. Marston, S., *Small molecule studies: the fourth wave of muscle research*. J  
658 *Muscle Res Cell Motil*, 2019. **40**(2): p. 69-76.
- 659 18. Risi, C., et al., *N-Terminal Domains of Cardiac Myosin Binding Protein C*  
660 *Cooperatively Activate the Thin Filament*. Structure, 2018. **26**(12): p. 1604-  
661 1611 e4.
- 662 19. Kirk, J.A., et al., *Pacemaker-induced transient asynchrony suppresses heart*  
663 *failure progression*. Sci Transl Med, 2015. **7**(319): p. 319ra207.

- 664 20. de Tombe, P.P. and G.J. Stienen, *Impact of temperature on cross-bridge*  
665 *cycling kinetics in rat myocardium*. J Physiol, 2007. **584**(Pt 2): p. 591-600.
- 666 21. Lin, B.L., et al., *Skeletal myosin binding protein-C isoforms regulate thin*  
667 *filament activity in a Ca(2+)-dependent manner*. Sci Rep, 2018. **8**(1): p. 2604.
- 668 22. Barrick, S.K., et al., *Computational Tool to Study Perturbations in Muscle*  
669 *Regulation and Its Application to Heart Disease*. Biophys J, 2019. **116**(12): p.  
670 2246-2252.
- 671 23. Westfall, M.V., et al., *Myofilament calcium sensitivity and cardiac disease:*  
672 *insights from troponin I isoforms and mutants*. Circ Res, 2002. **91**(6): p. 525-  
673 31.
- 674 24. Mamidi, R., et al., *Lost in translation: Interpreting cardiac muscle mechanics*  
675 *data in clinical practice*. Arch Biochem Biophys, 2019. **662**: p. 213-218.
- 676 25. Sheikh, F., et al., *Mouse and computational models link Mlc2v*  
677 *dephosphorylation to altered myosin kinetics in early cardiac disease*. J Clin  
678 Invest, 2012. **122**(4): p. 1209-21.
- 679 26. Phillips, S.A., D. Mirrlees, and P.J. Thornalley, *Modification of the glyoxalase*  
680 *system in streptozotocin-induced diabetic rats and the effect of the aldose*  
681 *reductase inhibitor Statil*. Biochem Soc Trans, 1993. **21**(2): p. 162S.
- 682 27. Dobler, D., et al., *Increased dicarbonyl metabolism in endothelial cells in*  
683 *hyperglycemia induces anoikis and impairs angiogenesis by RGD and*  
684 *GFOGER motif modification*. Diabetes, 2006. **55**(7): p. 1961-9.
- 685 28. Rabbani, N. and P.J. Thornalley, *Glyoxalase in diabetes, obesity and related*  
686 *disorders*. Semin Cell Dev Biol, 2011. **22**(3): p. 309-17.
- 687 29. Lo, T.W., et al., *Binding and modification of proteins by methylglyoxal under*  
688 *physiological conditions. A kinetic and mechanistic study with N alpha-*  
689 *acetylarginine, N alpha-acetylcysteine, and N alpha-acetyllysine, and bovine*  
690 *serum albumin*. J Biol Chem, 1994. **269**(51): p. 32299-305.
- 691 30. Lehman, W., R. Craig, and P. Vibert, *Ca(2+)-induced tropomyosin movement*  
692 *in Limulus thin filaments revealed by three-dimensional reconstruction*.  
693 Nature, 1994. **368**(6466): p. 65-7.
- 694 31. Vibert, P., R. Craig, and W. Lehman, *Steric-model for activation of muscle thin*  
695 *filaments*. J Mol Biol, 1997. **266**(1): p. 8-14.
- 696 32. McKillop, D.F. and M.A. Geeves, *Regulation of the interaction between actin*  
697 *and myosin subfragment 1: evidence for three states of the thin filament*.  
698 Biophys J, 1993. **65**(2): p. 693-701.
- 699 33. Clippinger, S.R., et al., *Disrupted mechanobiology links the molecular and*  
700 *cellular phenotypes in familial dilated cardiomyopathy*. Proc Natl Acad Sci U S  
701 A, 2019. **116**(36): p. 17831-17840.
- 702 34. Lo, T.W., T. Selwood, and P.J. Thornalley, *The reaction of methylglyoxal with*  
703 *aminoguanidine under physiological conditions and prevention of*  
704 *methylglyoxal binding to plasma proteins*. Biochem Pharmacol, 1994. **48**(10):  
705 p. 1865-70.
- 706 35. Ziolo, M.T., S.J. Dollinger, and G.M. Wahler, *Myocytes isolated from rejecting*  
707 *transplanted rat hearts exhibit reduced basal shortening which is reversible by*  
708 *aminoguanidine*. J Mol Cell Cardiol, 1998. **30**(5): p. 1009-17.
- 709 36. Nagy, L., et al., *The novel cardiac myosin activator omecamtiv mecarbil*  
710 *increases the calcium sensitivity of force production in isolated*  
711 *cardiomyocytes and skeletal muscle fibres of the rat*. Br J Pharmacol, 2015.  
712 **172**(18): p. 4506-4518.



- 713 37. Psotka, M.A., et al., *Cardiac Calcitropes, Myotropes, and Mitotropes: JACC*  
714 *Review Topic of the Week*. J Am Coll Cardiol, 2019. **73**(18): p. 2345-2353.
- 715 38. Pollesello, P., Z. Papp, and J.G. Papp, *Calcium sensitizers: What have we*  
716 *learned over the last 25 years?* Int J Cardiol, 2016. **203**: p. 543-8.
- 717 39. Alsulami, K. and S. Marston, *Small Molecules acting on Myofilaments as*  
718 *Treatments for Heart and Skeletal Muscle Diseases*. Int J Mol Sci, 2020.  
719 **21**(24).
- 720 40. Mun, J.Y., et al., *Myosin-binding protein C displaces tropomyosin to activate*  
721 *cardiac thin filaments and governs their speed by an independent mechanism*.  
722 Proc Natl Acad Sci U S A, 2014. **111**(6): p. 2170-5.
- 723 41. Herron, T.J., et al., *Activation of myocardial contraction by the N-terminal*  
724 *domains of myosin binding protein-C*. Circ Res, 2006. **98**(10): p. 1290-8.
- 725 42. Razumova, M.V., et al., *Contribution of the myosin binding protein C motif to*  
726 *functional effects in permeabilized rat trabeculae*. J Gen Physiol, 2008.  
727 **132**(5): p. 575-85.
- 728 43. Shaffer, J.F., R.W. Kensler, and S.P. Harris, *The myosin-binding protein C*  
729 *motif binds to F-actin in a phosphorylation-sensitive manner*. J Biol Chem,  
730 2009. **284**(18): p. 12318-27.
- 731 44. Boudina, S. and E.D. Abel, *Diabetic cardiomyopathy, causes and effects*. Rev  
732 Endocr Metab Disord, 2010. **11**(1): p. 31-9.
- 733 45. Jia, G., M.A. Hill, and J.R. Sowers, *Diabetic Cardiomyopathy: An Update of*  
734 *Mechanisms Contributing to This Clinical Entity*. Circ Res, 2018. **122**(4): p.  
735 624-638.
- 736 46. Viswanathan, M.C., et al., *Distortion of the Actin A-Triad Results in Contractile*  
737 *Disinhibition and Cardiomyopathy*. Cell Rep, 2017. **20**(11): p. 2612-2625.
- 738 47. Schmidt, W. and A. Cammarato, *The actin 'A-triad's' role in contractile*  
739 *regulation in health and disease*. J Physiol, 2019.
- 740 48. McNamara, J.W., et al., *The role of super-relaxed myosin in skeletal and*  
741 *cardiac muscle*. Biophys Rev, 2015. **7**(1): p. 5-14.
- 742 49. Stewart, M.A., et al., *Myosin ATP turnover rate is a mechanism involved in*  
743 *thermogenesis in resting skeletal muscle fibers*. Proc Natl Acad Sci U S A,  
744 2010. **107**(1): p. 430-5.
- 745 50. Woody, M.S., et al., *Positive cardiac inotrope omecamtiv mecarbil activates*  
746 *muscle despite suppressing the myosin working stroke*. Nat Commun, 2018.  
747 **9**(1): p. 3838.
- 748 51. Planelles-Herrero, V.J., et al., *Mechanistic and structural basis for activation*  
749 *of cardiac myosin force production by omecamtiv mecarbil*. Nat Commun,  
750 2017. **8**(1): p. 190.
- 751 52. Inchingolo, A.V., et al., *Revealing the mechanism of how cardiac myosin-*  
752 *binding protein C N-terminal fragments sensitize thin filaments for myosin*  
753 *binding*. Proc Natl Acad Sci U S A, 2019. **116**(14): p. 6828-6835.
- 754 53. Colson, B.A., et al., *Site-directed spectroscopy of cardiac myosin-binding*  
755 *protein C reveals effects of phosphorylation on protein structural dynamics*.  
756 Proc Natl Acad Sci U S A, 2016. **113**(12): p. 3233-8.
- 757 54. Gresham, K.S. and J.E. Stelzer, *The contributions of cardiac myosin binding*  
758 *protein C and troponin I phosphorylation to beta-adrenergic enhancement of*  
759 *in vivo cardiac function*. J Physiol, 2016. **594**(3): p. 669-86.
- 760 55. Li, J., et al., *AAV9 gene transfer of cMyBPC N-terminal domains ameliorates*  
761 *cardiomyopathy in cMyBPC-deficient mice*. JCI Insight, 2020. **5**(17).  
762